UQCRC1 downregulation impairs cognitive function in mice via AMPK inactivation (#114201)

First submission

Guidance from your Editor

Please submit by **8 Apr 2025** for the benefit of the authors (and your token reward) .

Structure and Criteria
Please read the 'Structure and Criteria' page for guidance.

Custom checks
Make sure you include the custom checks shown below, in your review.

Raw data check
Review the raw data.

Image check
Check that figures and images have not been inappropriately manipulated.

If this article is published your review will be made public. You can choose whether to sign your review. If uploading a PDF please remove any identifiable information (if you want to remain anonymous).

Files
Download and review all files from the materials page.

4 Figure file(s)
28 Raw data file(s)
1 Other file(s)

Custom checks

Vertebrate animal usage checks

Have you checked the authors ethical approval statement?

Were the experiments necessary and ethical?

Have you checked our animal research policies?

Structure and Criteria

Structure your review

The review form is divided into 5 sections. Please consider these when composing your review:

1. **BASIC REPORTING**
2. **EXPERIMENTAL DESIGN**
3. **VALIDITY OF THE FINDINGS**
4. General comments
5. Confidential notes to the editor

🗋 You can also annotate this PDF and upload it as part of your review

When ready submit online.

Editorial Criteria

Use these criteria points to structure your review. The full detailed editorial criteria is on your guidance page.

BASIC REPORTING

- Clear, unambiguous, professional English language used throughout.

- Intro & background to show context. Literature well referenced & relevant.

- Structure conforms to PeerJ standards, discipline norm, or improved for clarity.

- Figures are relevant, high quality, well labelled & described.

- Raw data supplied (see PeerJ policy).

EXPERIMENTAL DESIGN

- Original primary research within Scope of the journal.

- Research question well defined, relevant & meaningful. It is stated how the research fills an identified knowledge gap.

- Rigorous investigation performed to a high technical & ethical standard.

- Methods described with sufficient detail & information to replicate.

VALIDITY OF THE FINDINGS

- ℹ **Impact and novelty is not assessed.** Meaningful replication encouraged where rationale & benefit to literature is clearly stated.

- All underlying data have been provided; they are robust, statistically sound, & controlled.

- Conclusions are well stated, linked to original research question & limited to supporting results.

Standout reviewing tips

The best reviewers use these techniques

Tip	*Example*
Support criticisms with evidence from the text or from other sources	*Smith et al (J of Methodology, 2005, V3, pp 123) have shown that the analysis you use in Lines 241-250 is not the most appropriate for this situation. Please explain why you used this method.*
Give specific suggestions on how to improve the manuscript	*Your introduction needs more detail. I suggest that you improve the description at lines 57- 86 to provide more justification for your study (specifically, you should expand upon the knowledge gap being filled).*
Comment on language and grammar issues	*The English language should be improved to ensure that an international audience can clearly understand your text. Some examples where the language could be improved include lines 23, 77, 121, 128 – the current phrasing makes comprehension difficult. I suggest you have a colleague who is proficient in English and familiar with the subject matter review your manuscript, or contact a professional editing service.*
Organize by importance of the issues, and number your points	*1. Your most important issue* *2. The next most important item* *3. ...* *4. The least important points*
Please provide constructive criticism, and avoid personal opinions	*I thank you for providing the raw data, however your supplemental files need more descriptive metadata identifiers to be useful to future readers. Although your results are compelling, the data analysis should be improved in the following ways: AA, BB, CC*
Comment on strengths (as well as weaknesses) of the manuscript	*I commend the authors for their extensive data set, compiled over many years of detailed fieldwork. In addition, the manuscript is clearly written in professional, unambiguous language. If there is a weakness, it is in the statistical analysis (as I have noted above) which should be improved upon before Acceptance.*

UQCRC1 downregulation impairs cognitive function in mice via AMPK inactivation

Jing Zhang [1, 2], **Zuoxi Wu** [1], **Zonghong Long** [1], **Feng Ceng** [1], **Fuhai Bai** [Corresp., 1], **Hong Li** [Corresp. 1]

[1] Department of Anesthesiology, The Xinqiao Hospital, Army Medical University, Chongqing, China., Chongqing, Chongqing, China

[2] Department of Anesthesiology, Affiliated Hospital of North Sichuan Medical College, Nanchong, Sichuan, China., Nanchong, China

Corresponding Authors: Fuhai Bai, Hong Li
Email address: bfh@tmmu.edu.cn, lh78553@tmmu.edu.cn

Background: Ubiquinol-cytochrome c reductase core protein 1 (UQCRC1) is a subunit of complex III of the mitochondrial respiratory chain. Although earlier studies have indicated that UQCRC1 down-regulation causes cognitive impairment, the precise processes by which this happens are yet unknown.

Methods: In order to investigate its pathophysiological effects, we developed a mouse model with downregulated UQCRC1 expression. We evaluated hippocampal-dependent cognitive performance using behavioral paradigms. Then we quantified changes in bioenergetic state by ATP level measurements and oxidative stress utilizing reactive oxygen species (ROS) detection. AMP-activated protein kinase (AMPK) signaling dynamics and autophagic flux changes were assessed by molecular studies. Intervention strategies involving AMPK activation and lysosomal function potentiation were subsequently employed to elucidate mechanistic pathways.

Results: Our results show that UQCRC1 loss causes notable hippocampal-dependent cognitive deficits together with expected mitochondrial bioenergetics (lower ATP synthesis) and higher oxidative stress (more ROS buildup). Mechanistically, this phenotypic expression was linked to reduced AMPK activation and impaired autophagic flux. In UQCRC1 defective mice, pharmacological stimulation of AMPK or therapeutic potentiation of lysosomal activity essentially corrected cognitive deficits and restored mitochondrial redox equilibrium.

Conclusions: This work mechanistically defines AMPK as a fundamental metabolic orchestrator of mitochondrial-lysosomal functional crosstalk and reveals its non-canonical function in maintaining neuronal homeostasis via coordinated control of autophagic flux and redox balance. Our identification of AMPK-driven interoganelle communication as a modifiable treatment target creates a fresh paradigm for tackling cognitive decline originating in bioenergetic dysregulation.

UQCRC1 downregulation impairs cognitive function in mice via AMPK inactivation

Jing Zhang [1, 2], Zuoxi Wu[1], Zonghong Long[1], Ceng Feng[1], Fuhai Bai[1*], Hong Li[1*]

[1] Department of Anesthesiology, The Xinqiao Hospital, Army Medical University, Chongqing, China.

[2] Department of Anesthesiology, Affiliated Hospital of North Sichuan Medical College, Nanchong, Sichuan, China.

Corresponding Author:

Fuhai Bai, PhD.

Department of Anesthesiology, Second Affiliated Hospital of Army Medical University, PLA, No. 83 Xinqiao Road, Chongqing, 400037, China.

E-mail: bfh@tmmu.edu.cn

Hong Li, PhD.

Department of Anesthesiology, Second Affiliated Hospital of Army Medical University, PLA, No. 83 Xinqiao Road, Chongqing, 400037, China.

E-mail: lh78553@tmmu.edu.cn.

Abstract

Background: Ubiquinol-cytochrome c reductase core protein 1 (UQCRC1) is a subunit of complex III of the mitochondrial respiratory chain. Although earlier studies have indicated that UQCRC1 down-regulation causes cognitive impairment, the precise processes by which this happens are yet unknown.

Methods: In order to investigate its pathophysiological effects, we developed a mouse model with downregulated UQCRC1 expression. We evaluated hippocampal-dependent cognitive performance using behavioral paradigms. Then we quantified changes in bioenergetic state by ATP level measurements and oxidative stress utilizing reactive oxygen species (ROS) detection. AMP-activated protein kinase (AMPK) signaling dynamics and autophagic flux changes were assessed by molecular studies. Intervention strategies involving AMPK activation and lysosomal function potentiation were subsequently employed to elucidate mechanistic pathways.

Results: Our results show that UQCRC1 loss causes notable hippocampal-dependent cognitive deficits together with expected mitochondrial bioenergetics (lower ATP synthesis) and higher oxidative stress (more ROS buildup). Mechanistically, this phenotypic expression was linked to reduced AMPK activation and impaired autophagic flux. In UQCRC1 defective mice, pharmacological stimulation of AMPK or therapeutic potentiation of lysosomal activity essentially corrected cognitive deficits and restored mitochondrial redox equilibrium.

40   **Conclusions:** This work mechanistically defines AMPK as a fundamental metabolic
41   orchestrator of mitochondrial-lysosomal functional crosstalk and reveals its non-canonical
42   function in maintaining neuronal homeostasis via coordinated control of autophagic flux and
43   redox balance. Our identification of AMPK-driven interoganelle communication as a modifiable
44   treatment target creates a fresh paradigm for tackling cognitive decline originating in
45   bioenergetic dysregulation.
46
47

48   **Introduction**
49   In mammalian cells, mitochondria are the sites of energy metabolism and signal transmission.
50   They are thus crucial for cellular proliferation, autophagy, apoptosis, and differentiation (Zheng
51   et al., 2021; Zhou et al., 2018). The respiratory chain, a key structure responsible for ATP
52   generation, is composed of two electron carriers (ubiquinone and cytochrome c) and four
53   complexes (CI-CIV). In neurons, mitochondrial malfunction may cause an excessive buildup of
54   reactive oxygen species (ROS) and cytochrome c release into the cytoplasm. This subsequently
55   reduces ATP generation, modulates the activity of respiratory chain complexes I, II, and III, and
56   finally causes neuronal apoptosis and cognitive impairments (Fernandez-Vizarra & Zeviani,
57   2018a). Comprising two monomers, each with eleven subunits, Complex III of the respiratory
58   chain is a symmetric dimer. UQCRC1 is the fundamental protein required for the formation of
59   Complex III (Fernandez-Vizarra & Zeviani, 2018b). Previous research has shown that
60   downregulation of UQCRC1 expression might cause cognitive impairment (Shan et al., 2019).
61   Nonetheless, the underlying processes are still unknown.
62   Autophagy is a conserved process in eukaryotic evolution, which digests damaged organelles
63   or proteins and recycles them (Mizushima & Komatsu, 2011). Autophagy flux mainly includes
64   formation of autophagosomes, the fusion of autophagosomes with lysosomes, and the
65   degradation of autolysosome contents. Impairment of either step will result in impaired
66   autophagy flux (Levine & Kroemer, 2019; Liu et al., 2023). Mitophagy is the main mechanism
67   controlling the quantity and quality of mitochondria, which is essential for many life activities
68   such as homeostasis, proliferation, aging, apoptosis, etc., and is closely related to the occurrence
69   and development of neurodegenerative diseases, metabolic diseases, tumors, and other diseases
70   (Wang et al., 2023; Picca et al., 2023). After mitochondrial dystrophy or damage caused by
71   undesirable stimuli, it is labeled through various pathways, and LC3-II on the autophagosome
72   membrane recognizes and binds to the labeled mitochondria. Subsequently, autophagosomes
73   wrap the recognized mitochondria and fuse with lysosomes to degrade them. Abnormal
74   mitophagy in neurons can lead to a range of problems, such as metabolic disturbances, oxidative
75   stress, synaptic dysfunction, and calcium homeostasis imbalance (Katayama et al., 2020; Kerr et
76   al., 2017).
77   The AMP-activated protein kinase (AMPK) is an essential regulator and sensor of cellular
78   metabolism and stress responses. Triggers include energy stress, changes in cytoplasmic Ca2+
79   levels, and the presence of reactive oxygen species (ROS) (Trefts & Shaw, 2021). In several

80 ways, AMPK is involved in cellular homeostasis maintenance. It affects mitochondrial fusion
81 and fission, therefore regulating mitochondrial biogenesis and hence affecting mitochondrial
82 function (Virga et al., 2024; Herzig & Shaw, 2018). Moreover, AMPK plays a multifaceted role
83 in lysosomal biogenesis and function, hence supporting cellular homeostasis (Paquette et al.,
84 2021). AMPK therefore may be a fundamental protein linking mitochondrial malfunction to the
85 autophagy mechanism(Hu et al., 2021). Although earlier studies on mitophagy mostly
86 concentrate on how autophagy controls mitochondria, new investigations indicate that
87 mitochondria may potentially reciprocally control autophagy.

88   This study investigated the mechanistic role of UQCRC1 in cognitive regulation. Our findings
89 demonstrate that UQCRC1$^{+/-}$ mice showed hippocampal-dependent cognitive impairment along
90 with lower ATP generation, higher ROS levels, poor autophagy, and more hippocampal cell
91 apoptosis. Especially, our results underlined the important roles lysosomal and AMPK activation
92 play in these abnormalities.

93

Materials & Methods

94

Animals

95

96   C57BL/6 wild-type (WT) mice were provided by Charles River Laboratories (Chengdu, China)
97 and UQCRC1$^{+/-}$ heterozygous mice were generated by Professor Zhiyi Zuo (Shan et al., 2019),
98 with all animals housed under specific pathogen-free (SPF) conditions at Army Medical
99 University's animal facility. Mice (8-12 weeks old, 20-30 g) were maintained in standard cages
100 ($330 \times 210 \times 170$ mm; 5 mice/cage) with ad libitum access to food and water, under controlled
101 environmental parameters: 12-h light/dark cycle (08:00-20:00), 20-23 ℃ ambient temperature,
102 and 50-60% relative humidity.

103   Complemented by 16 female animals (8 UQCRC1$^{+/-}$ and 8 WT) for behavioral assessments,
104 this study included 36 male WT mice and 63 male UQCRC1$^{+/-}$ mice. After pre-treatment
105 behavioral testing, 8 WT and 8 UQCRC1$^{+/-}$ males were paired with 10 more genotype-matched
106 males (total n=18 per genotype) for hippocampus tissue collection at baseline. Six specimens per
107 genotype were assigned to ROS/ATP/caspase assays, six to Western blot analysis, and six to
108 transmission electron microscopy (TEM). The therapeutic evaluation phase consisted of 45
109 UQCRC1$^{+/-}$ males equally split into three treatment cohorts (solvent vehicle, A-769662, and
110 LH2-051). Eight mice per group received post-treatment behavioral assessment, with the
111 addition of 7 more mice per group (total n=15/group) for parallel tissue studies (six specimens
112 per group were assigned to ROS/ATP/caspase assays, three to Western blot analysis, and six to
113 TEM). For a comparison study, a separate cohort of 36 WT males followed identical
114 experimental schedules and tissue allocation guidelines.

115   Animals were euthanized prior to the planned endpoint only if they met predefined humane
116 endpoints. These criteria included (but were not limited to): severe weight loss (>20% of
117 baseline body weight) or failure to thrive; signs of irreversible distress or pain (e.g., labored
118 breathing, prolonged immobility, inability to access food/water); unexpected complications
119 directly related to the experimental intervention (e.g., neurological deficits). No animals required

120 early euthanasia in this study, as all subjects maintained stable health metrics within predefined
121 thresholds throughout the experimental timeline. No animals were retained beyond the study
122 period due to the terminal nature of the experimental design. Male subjects received 1% sodium
123 pentobarbital (50 mg/kg) intraperitoneally, while all female cohorts were euthanized following
124 behavioral assessment using gradual CO_2 asphyxiation (30%–99%, 15) with secondary
125 death confirmation. Randomization using random number tables ensured objective group
126 assignments, with sample sizes calculated by power analysis incorporating preliminary data and
127 literature benchmarks (Shan et al., 2019; Lin et al., 2020; Fernandez-Mosquera et al., 2019a;
128 Chen et al., 2022; Kim et al., 2021). The experimental protocol was developed prior to study
129 commencement and conducted in compliance with guidelines approved by the Army Medical
130 University's Laboratory Animal Welfare and Ethics Committee (Approval No.:
131 AMUWEC20245280; Approval date: 10/1/2024).
132
133 **Behavioral testing**
134   One week before the trials began, all the mice were adjusted to their surroundings. Every
135 behavioral test took place beginning at 10 am. Two hours before the start of every trial, mice
136 were allowed to become acquainted with the testing room. Different behavioral assessments
137 were kept one day apart. Following every test, the equipment was carefully cleaned with 75%
138 alcohol before the next one. Examiners left the room during testing to reduce outside influence.
139 EthoVision XT 11.5 (Noldus Inc., Netherlands) was used for data capture and analysis.
140 Novel Object Recognition test (NOR)
141   The ability of short-term memory in the hippocampus of mice was evaluated using the Novel
142 Object Recognition (NOR) test (Bevins & Besheer, 2006). The experimental setup consisted of
143 an acrylic rectangular enclosure (40 x 40 x 40 cm). The test comprised three separate phases.
144 Mice in the first step, the habituation phase, were allowed to explore freely for ten minutes in the
145 apparatus. Conducted 24 hours after habituation, in the second step, two identical objects
146 (Familiar Object, F) were symmetrically placed within the apparatus. Reintroduced into the
147 center area, mice had ten minutes to wander freely. Two hours after the second stage, in the third
148 stage of the novel-object test, one of the familiar items was substituted with a new object of the
149 same size but different form (Novel Object, N). Reintroduced into the center area, the mice were
150 allowed to search for another ten minutes. The time spent exploring the familiar object (tF) and
151 the novel object (tN) was recorded, and the recognition rate (RR) was calculated as follows: RR
152 $= tN / (tF + tN)$.
153 Nest Building test (NBT)
154   We used NBT to evaluate the general effect of UQCRC1 knockdown on hippocampally reliant
155 cognition. Experimental mice were individually housed in conventional cages with a single 2.5 g,
156 5 cm² tearable cotton pad and a tiny quantity of wood shavings on the day of the test at 6:00 PM.
157 Enough food and drink were offered. Photographs were taken the next day to record the nesting
158 activity, paying special attention to the degree to which the cotton pads were ripped and used in
159 nest building (Fig. 1C). After that, nesting quality was assessed and scored according to criteria

160 defined in earlier research (Deacon, 2006). Data from mice whose cotton pads were moist were
161 excluded from the analysis.
162 Barnes Maze
163   The Barnes maze test was a low-stress and effective way to evaluate spatial learning and
164 memory in mice. The apparatus consisted of a circular platform with 20 evenly spaced holes, one
165 of which was selected as the target hole. Under this hole was a detachable black box that
166 functioned as a sanctuary, enabling the mice to escape from lights and aural stimulation (Fig.
167 1E). Two stages comprised the test: the training phase and the testing phase. Mice positioned in
168 the middle of the labyrinth during the training period were watched for behavior. The test was
169 stopped when the mouse found and entered the black box or when the test lasted for three
170 minutes. Should a mouse fail to locate the box during this period, it was softly directed to the
171 black box and allowed to stay for one minute. Each mouse underwent three daily training
172 sessions for four consecutive days. The main performance indicator was the latency to enter the
173 black box. Conducted 24 hours after the last training session, the testing phase proceeded exactly
174 like the training phase. Performance measures for this phase were the latency to reach the black
175 box and the number of tries to find the box.
176 **Transmission Electron Microscope (TEM)**
177   Mice were initially perfused with ice-cold PBS. The hippocampus was carefully isolated and
178 sectioned into small fragments. The tissue samples were then fixed, dehydrated, infiltrated, and
179 immersed as required. Ultra-thin sections were prepared and stained with 2% uranyl acetate.
180 Quantitative analysis of the images was performed using ImageJ software (NIH,
181 https://imagej.nih.gov/ij/, version 1.54).
182 **Western Blotting**
183   The hippocampus was harvested and homogenized, and 20 μg of protein was loaded onto the
184 4–20% gels (ACE Biotechnology, cat# ET15420LGel) and then transferred to a PVDF
185 membrane using the Bio-Rad system. Membranes were blocked with a rapid blocking buffer
186 (MedChemExpress, cat# HY-K1027) for 10 minutes. The primary antibodies were incubated
187 overnight at 4°C. The main antibodies used were rabbit polyclonal anti-UCB (1:1000 dilution,
188 Abcam, cat# ab48394), rabbit polyclonal anti-AMPKα (1:1000 dilution, Cell Signaling
189 Technology, cat# 2532), and rabbit monoclonal anti-phospho-AMPKα (Thr172) (1:1000
190 dilution, Cell Signaling Technology, cat# 2535). After being diluted 1:3000 (ZSGB-BIO, cat#
191 ZB-2301), the HRP-conjugated goat anti-rabbit IgG was incubated at room temperature for one
192 hour. Images were processed using the ImageJ program (https://imagej.nih.gov/ij/, version 1.54)
193 for densitometric analysis.
194 **ATP Assay**
195   The method offered in the ATP content test kit handbook (Servicebio, cat# G4309-48T) was
196 followed to measure ATP content. Extracted hippocampal tissue was homogenized for lysis, was
197 boiled, cooled to room temperature. The sample was then centrifuged at $10,000 \times g$ for 15
198 minutes at 4°C. After obtaining the supernatant, 20 μL of supernatant was added to 100 μL of

199　ATP assay reagent and mixed thoroughly. The bioluminescent intensity was then assessed using

200　a luminometer (Fig. 2A). (Fig. 2A).

Assessment of reactive oxygen species (ROS)

202　Reactive oxygen species (ROS) levels were gauged using the ROS Detection Kit (Bestbio,

203　cat# BB-47051). The homogenate was centrifuged at 1000 g for three minutes at 4°C after the

204　hippocampal harvest and homogenization. Two μL of dihydroethidium (DHE) probe was then

205　added to 200 μL of supernatant and incubated in the dark at 37°C for thirty minutes. Measuring

206　fluorescence intensity at 510 nm as an excitation wavelength and 610 nm as an emission

207　wavelength. Calculating the ratio of fluorescence intensity to protein concentration to determine

208　the ROS levels in the tissue.

Assessment of Caspase 3 and Caspase 9

210　The Caspase 3/Caspase 9 Activity Assay Kit (made by MULTI SCIENCES, cat#

211　APC03/APC09) was used to evaluate the activation of caspase 3 and caspase 9. In a nutshell,

212　homogenized hippocampal tissue was centrifuged at 12,000 rpm for 15 minutes at 4 °C after

213　extraction. Following the directions on the kit, we collected the supernatant and made the

214　reaction mixture. After four hours of incubation at 37 °C, the samples were tested for absorbance

215　at 405 nm.

Intraperitoneal injection

217　UQCRC1$^{+/-}$ mice were randomly allocated into three groups: UQCRC1$^{+/-}$ + A-769662,

218　UQCRC1$^{+/-}$ + LH2-051, and UQCRC1$^{+/-}$ + solvent. Mice in the UQCRC1$^{+/-}$ + A-769662 and

219　UQCRC1$^{+/-}$ + LH2-051 cohorts received intraperitoneal injections of A-769662 (30 mg/kg,

220　MCE, cat# HY-50662) or LH2-051 (10 mg/kg, MCE, cat# HY-161723), respectively,

221　administered twice daily for a duration of 30 consecutive days. Mice in the UQCRC1$^{+/-}$ + solvent

222　group received an equivalent volume of solvent consisting of 10% DMSO, 40% PEG300, 5%

223　Tween-80, and 45% saline.

Statistical analysis

225　All experiments and analyses were performed under blinded conditions, with investigators

226　unaware of group allocations during both experimental procedures and data interpretation. All

227　acquired data were retained for statistical analysis without exclusion. The Shapiro-Wilk test was

228　employed to assess normality. Data conforming to a normal distribution were analyzed using

229　parametric tests, while non-parametric tests were applied to data that violated the normality

230　assumption. In the two-way ANOVA analysis, no outliers were detected using the method of

231　evaluating whether studentized residuals exceeded ±3. The Kruskal-Wallis H test, unpaired two-

232　tailed t-tests, Mann-Whitney U test, one-way ANOVA, and two-way ANOVA were used to

233　assess differences between groups. Statistical significance was defined as a p-value of less than

234　0.05. Data analysis was performed using GraphPad Prism (GraphPad Software, Boston, USA,

235　version 9.5) and SPSS (IBM, New York, USA, version 27.0). Statistical comparisons were

236　represented as *P < 0.05, **P < 0.01, ***P < 0.001, and ****P < 0.0001.

Results

The downregulation of UQCRC1 impaired cognitive function.

239   In the NOR, both male (Fig. 1B, p < 0.0001) and female (Fig. 1B, p < 0.05) UQCRC1$^{+/-}$ mice

240   demonstrated a markedly decreased recognition rate relative to WT controls. In the NBT, the

241   male UQCRC1$^{+/-}$ mice exhibited reduced performance (Fig. 1D, p < 0.01). From day 3 of the

242   Barnes maze training phase, the male UQCRC1$^{+/-}$ mice exhibited substantially longer escape

243   latencies (Fig. 1F, p < 0.05 on day 3, p < 0.01 on day 4). During the testing phase, male

244   UQCRC1$^{+/-}$ mice exhibited prolonged escape latencies (Fig. 1G, p < 0.05) and significantly

245   increased error rates (Fig. 1H, p < 0.05), whereas female UQCRC1$^{+/-}$ mice required more

246   attempts to find the target hole (Fig. 1H, p < 0.05). These results suggest that mitochondrial

247   dysfunction caused by the downregulation of UQCRC1 was strongly associated with cognitive

248   decline in male mice, while its effects on female mice were more variable. Thus, we focused on

249   male mice in the following research.

250   **The downregulation of UQCRC1 led to autophagy impairment.**

251   Our findings so far showed that the downregulation of UQCRC1 seriously reduced

252   hippocampally reliant cognitive capacities. We investigated this phenomenon further and

253   discovered a significant drop in ATP levels (Fig. 2B, p < 0.01) and a rise in ROS levels (Fig. 2C,

254   p < 0.05) in UQCRC1$^{+/-}$ mice. Autolysosomes (Fig. 2D, E, p < 0.05) were shown to be

255   accumulating along with rising LC3B II expression (Fig. 2F, G, p < 0.01). These results implied

256   that autophagy failure in mice followed from UQCRC1 downregulation. Previous research has

257   revealed that lysosomal malfunction in HeLa cells resulted from prolonged mitochondrial

258   respiratory chain failure reducing AMPK activation(Fernandez-Mosquera et al., 2019a). In

259   accordance with these results, our work showed that UQCRC1 downregulation resulted in a drop

260   in pAMPK levels (Fig. 2F, H, p < 0.00001) and a lower pAMPK/AMPK ratio (Fig. 2F, J, p <

261   0.00001), while total AMPK levels remained unchanged (Fig. 2F, I). These findings implied that

262   UQCRC1 downregulation reduceed hippocampal AMPK activation and impaired autolysosome

263   degradation. Notably, we observed an increase in the activation of caspase 3 (Fig. 2K, p <

264   0.0001) and caspase 9 (Fig. 2K, p < 0.001), which suggested that increased apoptosis in mice

265   resulted from UQCRC1 downregulation.

266   **Enhancing AMPK activity or improving lysosomal function ameliorated autophagy in**

267   **UQCRC1$^{+/-}$ mice.**

268   Our findings so far showed that the downregulation of UQCRC1 seriously reduced

269   hippocampally reliant cognitive capacities. We investigated this phenomenon further and

270   discovered a significant drop in ATP levels (Fig. 3B, p < 0.01) and a rise in ROS levels (Fig. 3C,

271   p < 0.05) in UQCRC1$^{+/-}$ mice. Autolysosomes (Fig. 3D, E, p < 0.05) were shown to be

272   accumulating along with rising LC3B II expression (Fig. 3F, G, p < 0.01). Furthermore, a rise in

273   the activation of caspase 3 (Fig. 3K, p < 0.0001) and caspase 9 (Fig. 3K, p < 0.001) was noted.

274   These results implied that autophagy failure and increased apoptosis in mice followed from

275   UQCRC1 downregulation. Previous research had revealed that lysosomal malfunction in HeLa

276   cells resulted from prolonged mitochondrial respiratory chain failure, reducing AMPK

277   activation. In accordance with these results, our work showed that UQCRC1 downregulation

278   resulted in a drop in pAMPK levels (Fig. 3F, H, p < 0.00001) and a lower pAMPK/AMPK ratio

279 (Fig. 3F, I, p < 0.00001), while total AMPK levels remained unchanged (Fig. 3F, J). These
280 findings implied that UQCRC1 downregulation reduced hippocampal AMPK activation and
281 impaired autolysosome degradation.
282 **Increasing AMPK activity or enhancing lysosomal function could both rescue cognitive**
283 **deficits in UQCRC1$^{+/-}$ mice.**
284 We performed behavioral evaluations after giving rescue therapy to investigate the potential
285 causal relationship between autophagy dysfunction and the cognitive abnormalities observed in
286 UQCRC1$^{+/-}$ mice. The findings indicated that augmenting AMPK activity or improving
287 lysosomal function markedly enhanced the performance of UQCRC1$^{+/-}$ mice in the new object
288 recognition test (Fig. 4A, B), nest-building test (Fig. 4C, D), and Barnes maze (Fig. 4E, F, G, H,
289 I). The results indicated that AMPK-mediated autophagy failure was pivotal in the cognitive
290 impairments linked to mitochondrial malfunction.

291 Discussion

292   Since UQCRC1-/- mice displayed embryonic lethality, UQCRC1 +/− mice were therefore
293 chosen as the experimental subjects. The brain, being a highly oxygen-consuming and energy-
294 demanding organ, requires a significant quantity of mitochondria to maintain its standard
295 functions. A multitude of studies have established that mitochondria can impact cognitive
296 abilities by modulating the functions of hippocampal neurons (Khacho et al., 2019; He et al.,
297 2022). Furthermore, extensive research has underscored the strong correlation between
298 mitochondrial activity and neurodegenerative disorders, including Alzheimer's disease (Wang et
299 al., 2020; Bishop et al., 2010). In this study, our findings showed that the downregulation of
300 UQCRC1 expression resulted in lower ATP levels and increased oxidative stress in the
301 hippocampal tissue. Moreover, this downregulation hampered autophagy flux by reducing
302 AMPK activity, which in turn resulted in increased neuronal apoptosis and contributed to
303 hippocampus-dependent cognitive dysfunction. This suggests that increasing AMPK activity or
304 improving autophagic flux may be a potential effective approach for treating cognitive decline
305 caused by mitochondrial dysfunction.
306   In the context of cognitive disorders associated with mitochondrial dysfunction, existing
307 research has highlighted a significant gender disparity. Before menopause, females appear to be
308 better equipped to combat oxidative stress due to their higher antioxidant defenses, which may
309 be attributed to the protective effects of estrogen (Viña & Borrás, 2010; Mandal et al., 2012;
310 Grimm et al., 2016). Consistent with these findings, our study also demonstrated that the
311 downregulation of UQCRC1 expression had a more pronounced and stable impact on males.
312 Therefore, in the mechanistic research section, we only used male mice to eliminate potential
313 confounding factors.
314   Autophagy has a complex and key role in neurons. It can keep the balance in neurons and help
315 neural functions work normally, but it might also cause harm to neurons in some situations
316 (Nixon & Rubinsztein, 2024). Produced during the start of autophagy, LC3II is a structural
317 protein linked to the autophagosome membrane that finally breaks down with the contents in the
318 autolysosome (Iriondo et al., 2022). Its expression degree exactly matches the count of
319 autophagosomes and autolysosomes. In this work, we found higher LC3II expression in
320 UQCRC1$^{+/-}$ mouse hippocampal tissue. Confirming a significant increase in the number of
321 autophagosomes/autolysosomes in this area, transmission electron microscopy also indicated

322 poor breakdown and recycling of autolysosomes in the hippocampal tissue of UQCRC1$^{+/-}$ mice.
323 Researchers have shown that LH2-051 significantly improves learning, memory, and cognitive
324 capacity in a mouse model of Alzheimer's disease (AD) via increasing lysosomal degradation
325 capability (Yin et al., 2023; Yin et al., 2023). This study found that LH2-051 greatly reduced
326 cognitive deficits in UQCRC1$^{+/-}$ mice, indicating that lysosomal dysfunction was a key
327 component of mitochondrial damage-induced cognitive impairments, and improving the function
328 of lysosomes was a targeted therapy.
329   While autophagy typically works to maintain cell survival by removing damaged components,
330 apoptosis is triggered when the damage is beyond repair. Apoptosis is a controlled and
331 physiological type of cell apoptosis that happens under certain physiological or pathological
332 conditions. It is controlled by genetic pathways (Renehan et al., 2001; Bredesen, 1995).
333 Mitochondria play a crucial role in the apoptotic pathway, and dysfunctional mitochondria can
334 trigger apoptosis via multiple pathways. The main events that initiate the cascade include the
335 release of cytochrome c and the apoptosis-inducing factor (AIF) and the excessive opening of the
336 mitochondrial permeability transition pore (mPTP). Reduced ATP content and elevated reactive
337 oxygen species (ROS) can make neurons more sensitive to apoptosis-related proteins, which
338 speed up the process (Nguyen et al., 2023; Bock & Tait, 2020). In this work, we found out that
339 more neural apoptosis in the hippocampal tissue made the cognitive ability worse in UQCRC1$^{+/-}$
340 mice.
341   AMPK is a highly conserved protein kinase and a major responder to mitochondrial stress,
342 which is very sensitive to changes in the ratio of AMP to ATP. Taking out ndufs4, which is a
343 subunit of respiratory chain complex I, has been shown to lower AMPK activation in the brain
344 (Fernandez-Mosquera et al., 2019b). Previous studies have also shown that AMPK was involved
345 in lysosome formation in vitro and in living organisms (Cheng et al., 2021; Alers et al., 2012;
346 Patra et al., 2019). In this study, we also demonstrated that via AMPK-mediated processes,
347 mitochondrial malfunction caused autolysosomes accumulation. Together, AMPK might be an
348 important mediator between mitochondrial dysfunction and an altered autophagy flux.
349   There are various limits to this research that need thought. First, our studies indicated sex-
350 dependent different effects of UQCRCR1 downregulation on murine cognitive function, while
351 the underlying mechanisms are still unknown. Second, while behavioral assessments
352 preliminarily identified the hippocampus as the primary affected region, given the widespread
353 neuronal network underpinning cognitive processes it is impossible to completely eliminate
354 possible involvement from extra-hippocampal locations. Thirdly, although we demonstrated that
355 UQCRCR1-mediated mitochondrial dysfunction impairs cognition through AMPK-dependent
356 autophagic dysregulation, two critical mechanistic gaps persist: 1) the precise signaling cascades
357 linking AMPK activation to autophagic modulation, and 2) the exact neurobiological
358 mechanisms through which autophagy perturbations mediate cognitive deficits.
359
360 **Conclusions**

361   The brain depends primarily on oxygen and energy, hence it needs significant mitochondrial
362   reserves to maintain normal physiological operations. Because of its increased metabolic needs,
363   limited vascular reserve, and unique synaptic plasticity properties, the hippocampus region
364   shows especially sensitivity to hypoxic-ischemic damage and is thus a target of great importance
365   for neuroprotective treatments. This work shows that in mouse models UQCRC1 deficiency
366   causes hippocampus dependent cognitive impairment. UQCRC1 downregulation has been shown
367   in subsequent studies to cause a cascade of pathological changes in the hippocampal cells
368   including lowered ATP synthesis capacity, reduced AMPK activation ratio, along with elevated
369   ROS accumulation, decreased autophagolysosome density, and caspase-3 and caspase-9
370   enhanced activation. By means of pharmacological therapies in UQCRC1$^{+/-}$ mice, we found that
371   lysosomal enhancement by LH2-051 therapy and AMPK activation by intraperitoneal A-769662
372   essentially corrected cognitive abnormalities. Especially, AMPK potentiation greatly reduced
373   autophagolysosome accumulation, but lysosomal modification had little effect on AMPK activity
374   in turn. These results define a molecular route wherein UQCRC1 deficiency-mediated
375   mitochondrial dysfunction aggravates neuronal apoptosis via lysosomal impairment in the
376   hippocampal region with AMPK acting as a central regulating hub. This cascade offers fresh
377   treatment options for reducing cognitive impairment linked with mitochondrial diseases.
378

Acknowledgements

The UQCRC1$^{+/-}$ mice were offered by Professor Zhiyi Zuo's laboratory (University of Virginia). We are very grateful for that.

References

Alers, S., Löffler, A.S., Wesselborg, S., and Stork, B. 2012. Role of AMPK-mTOR-Ulk1/2 in the regulation of autophagy: cross talk, shortcuts, and feedbacks. MOLECULAR AND CELLULAR BIOLOGY 32:2-11. 10.1128/MCB.06159-11

Bevins, R.A., and Besheer, J. 2006. Object recognition in rats and mice: a one-trial non-matching-to-sample learning task to study 'recognition memory'. Nature Protocols 1:1306-1311. 10.1038/nprot.2006.205

Bishop, N.A., Lu, T., and Yankner, B.A. 2010. Neural mechanisms of ageing and cognitive decline. NATURE 464:529-535. 10.1038/nature08983

Bock, F.J., and Tait, S.W.G. 2020. Mitochondria as multifaceted regulators of cell death. NATURE REVIEWS MOLECULAR CELL BIOLOGY 21:85-100. 10.1038/s41580-019-0173-8

Bredesen, D.E. 1995. Neural apoptosis. ANNALS OF NEUROLOGY 38:839-851. 10.1002/ana.410380604

Chen, Y., Liu, L., Xia, L., Wu, N., Wang, Y., Li, H., Chen, X., Zhang, X., Liu, Z., Zhu, M., Liao, Q., and Wang, J. 2022. TRPM7 silencing modulates glucose metabolic reprogramming to inhibit the growth of ovarian cancer by enhancing AMPK activation to promote HIF-1α degradation. JOURNAL OF EXPERIMENTAL & CLINICAL CANCER RESEARCH 41:44. 10.1186/s13046-022-02252-1

Cheng, A., Tse, K., Chow, H., Gan, Y., Song, X., Ma, F., Qian, Y.X.Y., She, W., and Herrup, K. 2021. ATM loss disrupts the autophagy-lysosomal pathway. Autophagy 17:1998-2010. 10.1080/15548627.2020.1805860

Deacon, R.M.J. 2006. Assessing nest building in mice. Nature Protocols 1:1117-1119. 10.1038/nprot.2006.170

Fernandez-Mosquera, L., Yambire, K.F., Couto, R., Pereyra, L., Pabis, K., Ponsford, A.H., Diogo, C.V., Stagi, M., Milosevic, I., and Raimundo, N. 2019a. Mitochondrial respiratory chain deficiency inhibits lysosomal hydrolysis. Autophagy 15:1572-1591. 10.1080/15548627.2019.1586256

Fernandez-Mosquera, L., Yambire, K.F., Couto, R., Pereyra, L., Pabis, K., Ponsford, A.H., Diogo, C.V., Stagi, M., Milosevic, I., and Raimundo, N. 2019b. Mitochondrial respiratory chain deficiency inhibits lysosomal hydrolysis. Autophagy 15:1572-1591. 10.1080/15548627.2019.1586256

Fernandez-Vizarra, E., and Zeviani, M. 2018. Mitochondrial complex III Rieske Fe-S protein processing and assembly. CELL CYCLE 17:681-687. 10.1080/15384101.2017.1417707

Grimm, A., Mensah-Nyagan, A.G., and Eckert, A. 2016. Alzheimer, mitochondria and gender. NEUROSCIENCE AND BIOBEHAVIORAL REVIEWS 67:89-101. 10.1016/j.neubiorev.2016.04.012

419   He, K., Zhang, J., Zhang, W., Wang, S., Li, D., Ma, X., Wu, X., Chai, X., and Liu, Q. 2022.

420   Hippocampus-Based Mitochondrial Respiratory Function Decline Is Responsible for

421   Perioperative Neurocognitive Disorders. Frontiers in Aging Neuroscience 14:772066.

422   10.3389/fnagi.2022.772066

423   Herzig, S., and Shaw, R.J. 2018. AMPK: guardian of metabolism and mitochondrial homeostasis.

424   NATURE REVIEWS MOLECULAR CELL BIOLOGY 19:121-135. 10.1038/nrm.2017.95

425   Hu, Y., Chen, H., Zhang, L., Lin, X., Li, X., Zhuang, H., Fan, H., Meng, T., He, Z., Huang, H.,

426   Gong, Q., Zhu, D., Xu, Y., He, P., Li, L., and Feng, D. 2021. The AMPK-MFN2 axis regulates

427   MAM dynamics and autophagy induced by energy stresses. Autophagy 17:1142-1156.

428   10.1080/15548627.2020.1749490

429   Iriondo, M.N., Etxaniz, A., Varela, Y.R., Ballesteros, U., Hervás, J.H., Montes, L.R., Goñi, F.M.,

430   and Alonso, A. 2022. LC3 subfamily in cardiolipin-mediated mitophagy: a comparison of the

431   LC3A, LC3B and LC3C homologs. Autophagy 18:2985-3003.

432   10.1080/15548627.2022.2062111

433   Katayama, H., Hama, H., Nagasawa, K., Kurokawa, H., Sugiyama, M., Ando, R., Funata, M.,

434   Yoshida, N., Homma, M., Nishimura, T., Takahashi, M., Ishida, Y., Hioki, H., Tsujihata, Y., and

435   Miyawaki, A. 2020. Visualizing and Modulating Mitophagy for Therapeutic Studies of

436   Neurodegeneration. CELL 181:1176-1187. 10.1016/j.cell.2020.04.025

437   Kerr, J.S., Adriaanse, B.A., Greig, N.H., Mattson, M.P., Cader, M.Z., Bohr, V.A., and Fang, E.F.

438   2017. Mitophagy and Alzheimer's Disease: Cellular and Molecular Mechanisms. TRENDS IN

439   NEUROSCIENCES 40:151-166. 10.1016/j.tins.2017.01.002

440   Khacho, M., Harris, R., and Slack, R.S. 2019. Mitochondria as central regulators of neural stem

441   cell fate and cognitive function. NATURE REVIEWS NEUROSCIENCE 20:34-48.

442   10.1038/s41583-018-0091-3

443   Kim, S., Lee, J., Shin, S.G., Kim, J.K., Silwal, P., Kim, Y.J., Shin, N., Kim, P.S., Won, M., Lee,

444   S., Kim, S.Y., Sasai, M., Yamamoto, M., Kim, J., Bae, J., and Jo, E. 2021. ESRRA (estrogen

445   related receptor alpha) is a critical regulator of intestinal homeostasis through activation of

446   autophagic flux via gut microbiota. Autophagy 17:2856-2875. 10.1080/15548627.2020.1847460

447   Levine, B., and Kroemer, G. 2019. Biological Functions of Autophagy Genes: A Disease

448   Perspective. CELL 176:11-42. 10.1016/j.cell.2018.09.048

449   Lin, C., Tsai, P., Lin, H., Hattori, N., Funayama, M., Jeon, B., Sato, K., Abe, K., Mukai, Y.,

450   Takahashi, Y., Li, Y., Nishioka, K., Yoshino, H., Daida, K., Chen, M., Cheng, J., Huang, C.,

451   Tzeng, S., Wu, Y., Lai, H., Tsai, H., Yen, R., Lee, N., Lo, W., Hung, Y., Chan, C., Ke, Y., Chao,

452   C., Hsieh, S., Farrer, M., and Wu, R. 2020. Mitochondrial UQCRC1 mutations cause autosomal

453   dominant parkinsonism with polyneuropathy. BRAIN 143:3352-3373. 10.1093/brain/awaa279

454   Liu, S., Yao, S., Yang, H., Liu, S., and Wang, Y. 2023. Autophagy: Regulator of cell death. Cell

455   Death & Disease 14:648. 10.1038/s41419-023-06154-8

456   Mandal, P.K., Tripathi, M., and Sugunan, S. 2012. Brain oxidative stress: detection and mapping

457   of anti-oxidant marker 'Glutathione' in different brain regions of healthy male/female, MCI and

458   Alzheimer patients using non-invasive magnetic resonance spectroscopy. BIOCHEMICAL AND
459   BIOPHYSICAL RESEARCH COMMUNICATIONS 417:43-48. 10.1016/j.bbrc.2011.11.047
460   Mizushima, N., and Komatsu, M. 2011. Autophagy: renovation of cells and tissues. CELL
461   147:728-741. 10.1016/j.cell.2011.10.026
462   Nguyen, T.T., Wei, S., Nguyen, T.H., Jo, Y., Zhang, Y., Park, W., Gariani, K., Oh, C., Kim,
463   H.H., Ha, K., Park, K.S., Park, R., Lee, I., Shong, M., Houtkooper, R.H., and Ryu, D. 2023.
464   Mitochondria-associated programmed cell death as a therapeutic target for age-related disease.
465   EXPERIMENTAL AND MOLECULAR MEDICINE 55:1595-1619. 10.1038/s12276-023-
466   01046-5
467   Nixon, R.A., and Rubinsztein, D.C. 2024. Mechanisms of autophagy-lysosome dysfunction in
468   neurodegenerative diseases. NATURE REVIEWS MOLECULAR CELL BIOLOGY 25:926-946.
469   10.1038/s41580-024-00757-5
470   Paquette, M., El-Houjeiri, L., C Zirden, L., Puustinen, P., Blanchette, P., Jeong, H., Dejgaard, K.,
471   Siegel, P.M., and Pause, A. 2021. AMPK-dependent phosphorylation is required for
472   transcriptional activation of TFEB and TFE3. Autophagy 17:3957-3975.
473   10.1080/15548627.2021.1898748
474   Patra, K.C., Weerasekara, V.K., and Bardeesy, N. 2019. AMPK-Mediated Lysosome Biogenesis
475   in Lung Cancer Growth. Cell Metabolism 29:238-240. 10.1016/j.cmet.2018.12.011
476   Picca, A., Faitg, J., Auwerx, J., Ferrucci, L., and D'Amico, D. 2023. Mitophagy in human health,
477   ageing and disease. Nature Metabolism 5:2047-2061. 10.1038/s42255-023-00930-8
478   Renehan, A.G., Booth, C., and Potten, C.S. 2001. What is apoptosis, and why is it important?
479   BMJ-British Medical Journal 322:1536-1538. 10.1136/bmj.322.7301.1536
480   Shan, W., Li, J., Xu, W., Li, H., and Zuo, Z. 2019. Critical role of UQCRC1 in embryo survival,
481   brain ischemic tolerance and normal cognition in mice. CELLULAR AND MOLECULAR
482   LIFE SCIENCES 76:1381-1396. 10.1007/s00018-019-03007-6
483   Trefts, E., and Shaw, R.J. 2021. AMPK: restoring metabolic homeostasis over space and time.
484   MOLECULAR CELL 81:3677-3690. 10.1016/j.molcel.2021.08.015
485   Viña, J., and Borrás, C. 2010. Women live longer than men: understanding molecular
486   mechanisms offers opportunities to intervene by using estrogenic compounds.
487   ANTIOXIDANTS & REDOX SIGNALING 13:269-278. 10.1089/ars.2009.2952
488   Virga, D.M., Hamilton, S., Osei, B., Morgan, A., Kneis, P., Zamponi, E., Park, N.J., Hewitt, V.L.,
489   Zhang, D., Gonzalez, K.C., Russell, F.M., Grahame Hardie, D., Prudent, J., Bloss, E., Losonczy,
490   A., Polleux, F., and Lewis, T.L.J. 2024. Activity-dependent compartmentalization of dendritic
491   mitochondria morphology through local regulation of fusion-fission balance in neurons in vivo.
492   Nature Communications 15:2142. 10.1038/s41467-024-46463-w
493   Wang, S., Long, H., Hou, L., Feng, B., Ma, Z., Wu, Y., Zeng, Y., Cai, J., Zhang, D., and Zhao, G.
494   2023. The mitophagy pathway and its implications in human diseases. Signal Transduction and
495   Targeted Therapy 8:304. 10.1038/s41392-023-01503-7

496   Wang, W., Zhao, F., Ma, X., Perry, G., and Zhu, X. 2020. Mitochondria dysfunction in the

497   pathogenesis of Alzheimer's disease: recent advances. Molecular Neurodegeneration 15:30.

498   10.1186/s13024-020-00376-6

499   Yin, L., Zhou, J., Li, T., Wang, X., Xue, W., Zhang, J., Lin, L., Wang, N., Kang, X., Zhou, Y.,

500   Liu, H., and Li, Y. 2023. Inhibition of the dopamine transporter promotes lysosome biogenesis

501   and ameliorates Alzheimer's disease-like symptoms in mice. Alzheimers & Dementia 19:1343-

502   1357. 10.1002/alz.12776

503   Yin, L., Zhou, Y., Liu, H., and Li, Y. 2023. LYECs: lysosome-enhancing compounds as

504   potential therapeutic approaches for Alzheimer disease. Autophagy 19:1863-1864.

505   10.1080/15548627.2022.2131247

506   Zheng, X., Li, W., Xu, H., Liu, J., Ren, L., Yang, Y., Li, S., Wang, J., Ji, T., and Du, G. 2021.

507   Sinomenine ester derivative inhibits glioblastoma by inducing mitochondria-dependent

508   apoptosis and autophagy by PI3K/AKT/mTOR and AMPK/mTOR pathway. Acta

509   Pharmaceutica Sinica B 11:3465-3480. 10.1016/j.apsb.2021.05.027

510   Zhou, Z., Austin, G.L., Young, L.E.A., Johnson, L.A., and Sun, R. 2018. Mitochondrial

511   Metabolism in Major Neurological Diseases. Cells 7. 10.3390/cells7120229

Figure 1

The downregulation of *UQCRC1* impaired cognitive function.

(A) Schematic representation of NOR, created in https://BioRender.com. (B) The recognition rate of both male and female *UQCRC1* +/- mice was lower than that of their conspecifics (n=8). (C) Schematic representation of NBT, created in https://BioRender.com . (D) The nesting score of male *UQCRC1* +/- mice was lower (n=8). (E) Schematic representation of the Barnes maze, created in https://BioRender.com . (F) Comapared to male WT mice, male *UQCRC1* +/- mice exhibited longer escape latencies from day 3 during the training phase of Barnes maze (n=8) . (G) Male *UQCRC1* +/- mice had prolonged escape latencies during the testing phase of the Barnes maze (n=8) . (H) Both male and female *UQCRC1* +/- mice took more attempts to find the correct hole (n=8) . Recognition rate in NOR and escape latencies in both the training and testing phases of the Barnes maze were quantified and expressed as mean ± standard error of the mean (SEM). N esting score in NBT and the numbers to identify target box during Barnes maze were recorded and presented using non-parametric descriptors (median with interquartile range). ****$p < 0.0001$; **$p < 0.01$; *$p < 0.05$.
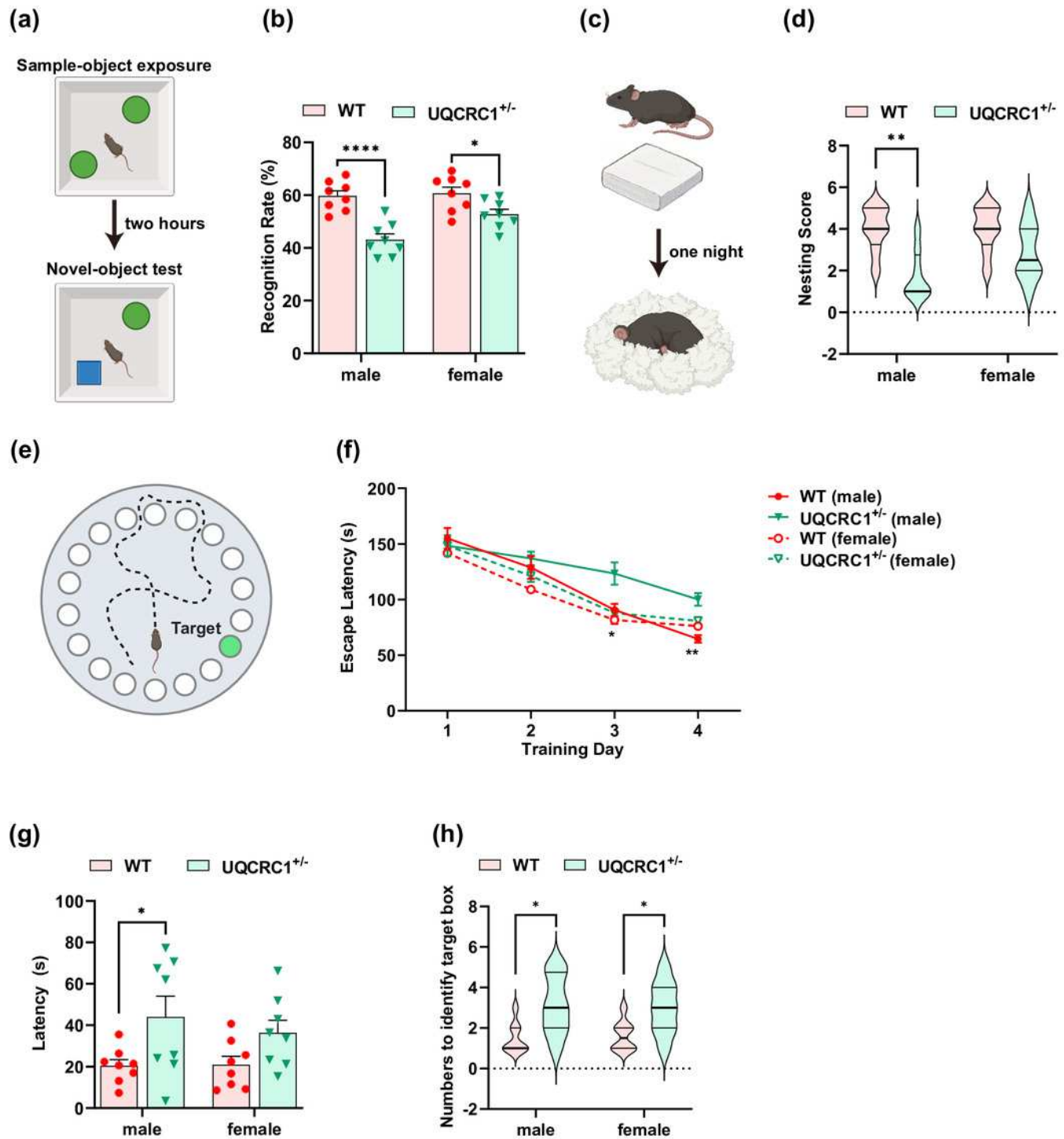
Figure 2

The downregulation of *UQCRC1* led to autophagy impairment.

(A) Schematic illustration of the experimental design for ATP assays, reactive oxygen species assessments, and caspase 3 and caspase 9 evaluations, created in https://BioRender.com .
(B) The ATP level in *UQCRC1* +/- mice was lower. (C) The ROS level in *UQCRC1* +/- mice was higher. (D) Representative transmission electron microscope (TEM) images of WT mice and *UQCRC1* +/- mice (red arrows indicate autolysosomes; scale bar: 2 μm). (E) The density of autolysosomes was higher in *UQCRC1* +/- mice. (F) Western blot images of LC3B I, LC3B II, pAMPK, AMPK in WT mice and *UQCRC1* +/- mice. (G-H) Quantification of protein expression of LC3B II (G), pAMPK (H), AMPK (I) and pAMPK/AMPK ratio (J). (K) Activation of both caspase 3 and caspase 9 was higher in *UQCRC1* +/- mice. Data are represented as mean ± SEM. ****$p < 0.0001$; ***$p < 0.001$; **$p < 0.01$; *$p < 0.05$.
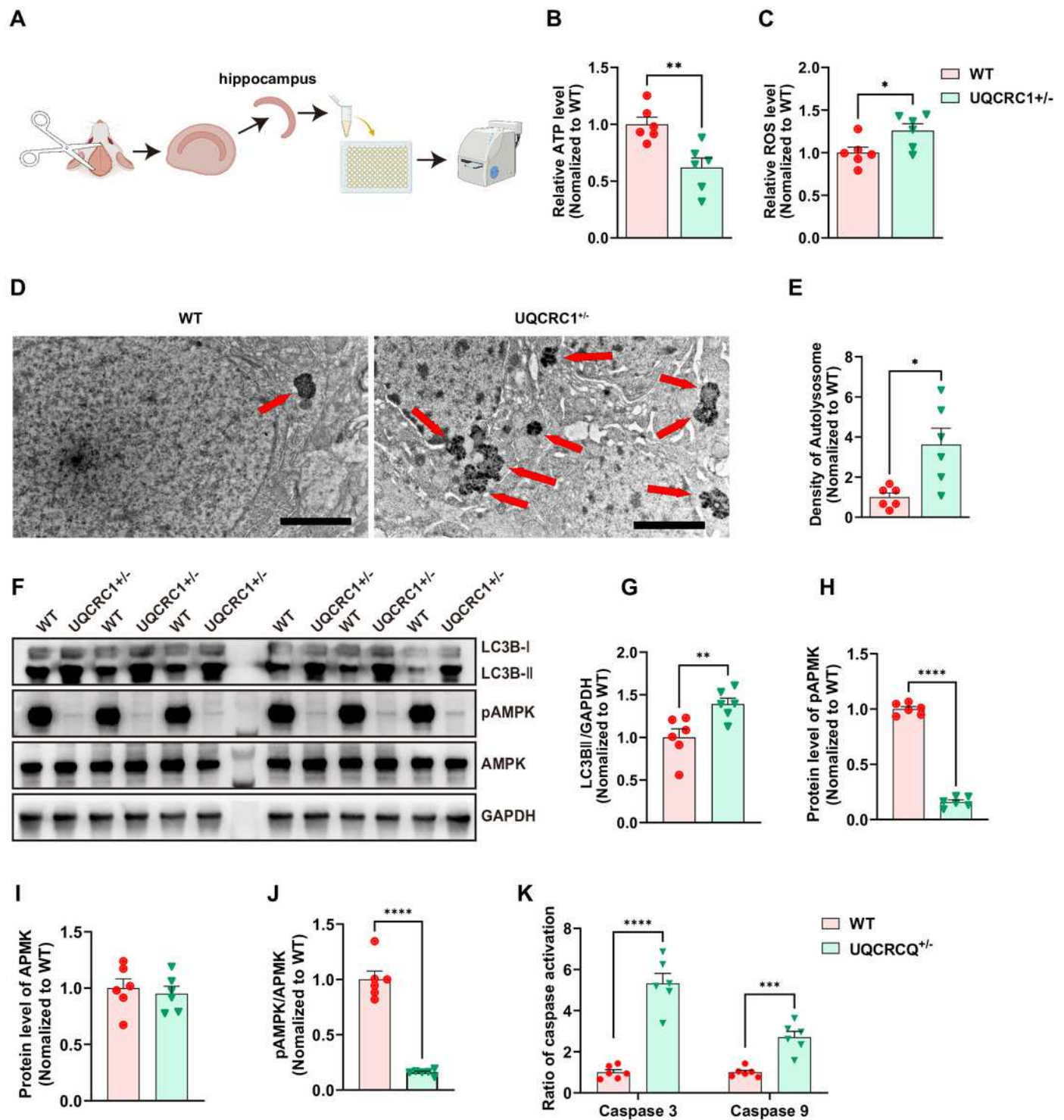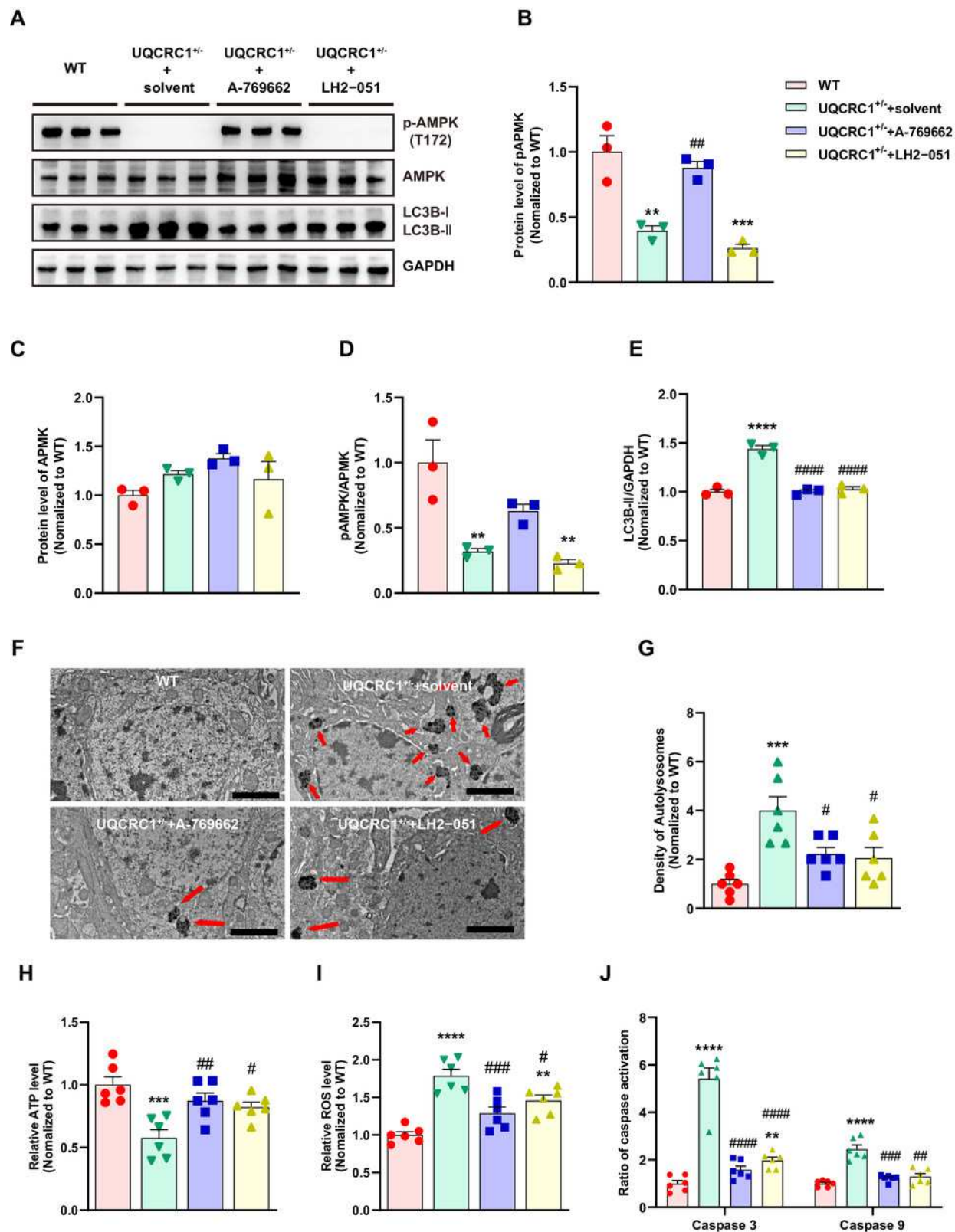
Figure 3

Both lysosomal function improvement and AMPK activity enhancement ameliorated autophagy in *UQCRC1* mice.

(A) Western blot image of pAMPK, AMPK, LC3B I and LC3B Ⅱ. (B-E) Quantification of protein expression of pAMPK (B), AMPK (C), pAMPK/AMPK (D) and LC3B Ⅱ (E) . (F) Representative transmission electron microscope (TEM) images (red arrows indicate autolysosomes; scale bar: 2 μm). (G) The density of a utolysosomes in *UQCRC1* +/- mice reduced after the administration of A-769662 or LH2-051. (H) The ATP level in *UQCRC1* +/- mice increased after the administration of A-769662 or LH2-051. (I) The ROS levels in *UQCRC1* +/- mice diminished following the treatment with A-769662 or LH2-051; however, after LH2-051 administration, the ROS levels did not return to those observed in WT mice. (J) Following administration of A-769662 or LH2-051, activation of caspase 3 and caspase 9 in *UQCRC1* +/- mice was reduced; however, caspase 3 activation did not recover to WT levels after LH2-051 treatment. Data are represented as mean ± SEM. **** $p < 0.0001$ vs. WT; *** $p < 0.001$ vs. WT; ** $p < 0.01$ vs. WT. #### $p < 0.0001$ vs. UQCRC1 +/- +solvent; ### $p < 0.001$ vs. UQCRC1 +/- +solvent; ## $p < 0.01$ vs. UQCRC1 +/- +solvent; # $p < 0.05$ vs. UQCRC1 +/- +solvent.

Figure 4

The cognitive deficits in *UQCRC1* +/- mice were ameliorated by augmenting AMPK activation and improving lysosomal function.

(A) Representative heat maps showing the duration and location of the subject during novel object recognition ("N" and "F" represent novel object and familiar object, respectively). (B) The recognition rate of *UQCRC1* +/- mice increased after the administration of A-769662 or LH2-051. (C) Representative figures of the nest-building test. (D) The nesting score of *UQCRC1* +/- mice increased after the administration of A-769662 or LH2-051. (E) Representative trajectory chart during testing phase of the Barnes maze (gray circle indicates the target hole). (F) Over the training phase of the Barnes maze, the escape latencies of *UQCRC1* +/- mice were restored to levels similar to WT mice. (G) A-769662 or LH2-051 treatment lowered the escape latencies of *UQCRC1* +/- mice during the Barnes maze testing phase. (H) *UQCRC1* +/- mice treated with A-769662 or LH2-051 showed fewer attempts to find the target hole. Recognition rate in NOR and escape latencies in both the training and testing phases of the Barnes maze were quantified and expressed as mean ± SEM. Nesting score in NBT and the numbers to identify target box during Barnes maze were presented as median and interquartile range. **** $p < 0.0001$ vs. WT; ** $p < 0.01$ vs. WT, * $p < 0.05$ vs. WT. ### $p < 0.001$ vs. UQCRC1 +/- +solvent; ## $p < 0.01$ vs. UQCRC1 +/- +solvent; # $p < 0.05$ vs. UQCRC1 +/- +solvent.